Journal of Visualized Experiments

In Situ Transmission Electron Microscopy with Biasing and Fabrication of Asymmetric Crossbars Based on Mixed-Phased a-VOx

--Manuscript Draft--

Article Type:	Invited Methods Article - JoVE Produced Video
Manuscript Number:	JoVE61026R2
Full Title:	In Situ Transmission Electron Microscopy with Biasing and Fabrication of Asymmetric Crossbars Based on Mixed-Phased a-VOx
Section/Category:	JoVE Engineering
Keywords:	in situ transmission electron microscopy, nanostructural analysis, amorphous vanadium oxide, resistive switching, volatile threshold switching, crossbars
Corresponding Author:	Shruti Nirantar RMIT University College of Science Engineering and Health Melbourne, VIC AUSTRALIA
Corresponding Author's Institution:	RMIT University College of Science Engineering and Health
Corresponding Author E-Mail:	shruti.nirantar@gmail.com
Order of Authors:	Shruti Nirantar, M.S
	Edwin Mayes
	Sharath Sriram
Additional Information:	
Question	**Response**
Please indicate whether this article will be Standard Access or Open Access.	Standard Access (US$2,400)
Please indicate the **city, state/province, and country** where this article will be **filmed**. Please do not use abbreviations.	Melbourne, Victoria, Australia

November 14, 2019

Functional Materials and Microsystems Research Group
GPO Box 2476
Melbourne VIC 3001
Australia
Tel. + 61 3 9925 0440
www.rmit.edu.au

To
Benjamin Werth
Senior Science Editor
JoVE

Dear Benjamin Werth,

We are pleased to submit our invited manuscript entitled "Fabrication process and *in situ* nanostructural analysis methodology of volatile threshold switching in mixed-phased *a*-VO_x based asymmetric crossbars" for consideration for publication in *JoVE*.

Nanoscale resistive memories are building blocks for future energy-efficient logic technology and brain-inspired neuromorphic computing hardware. Creating memory elements and understanding its operation mechanisms that can be programmed to demonstrate different switching performance – optimised either for logic or neuromorphics or for performance or energy efficiency – is critical to advancements in this field.

In this work, we demonstrate complete fabrication process and the methodology of transmission electron microscopy analysis with *in situ* biasing in the cross-point device structure. The representative results used here from this experiment are already published in *Advanced Electronics Materials* entitled as "*In situ* nanostructural analysis of volatile threshold switching and nano-volatile bipolar resistive switching in a mixed-phase *a*-VO_x asymmetric crossbars".

Our findings demonstrate an experimental procedure which has significant impact in the field of resistive random access memories (RRAM) to study the nanostructural changes visually *in situ*. This can reveal the underlying mechanisms with reliable evidences and develop significant understanding of the device behaviours.

We believe that our video manuscript will appeal to the diverse group of researchers from resistive random-access memories, nanoelectronics, green electronics, thin film material science, physics, and electron microscopists.

Each author herein confirms that methodology part of this work has not been previously published in any peer-reviewed journal and is not currently under consideration by any other journal. However, the representative results used here are already published which have been reference correctly and reuse permissions have been received. All authors have substantially contributed to the research activities and in preparation of this manuscript. Finally, we declare no competing financial interests.

Yours sincerely,

Shruti Nirantar
PhD Candidate

Functional Materials and Microsystems research group
School of Engineering
RMIT University
Phone +61-470622797 (Mobile)
E-mail shruti.nirantar@gmail.com

TITLE:

In Situ Transmission Electron Microscopy with Biasing and Fabrication of Asymmetric Crossbars Based on Mixed-Phased *a*-VO_x

AUTHORS AND AFFILIATIONS:

Shruti Nirantar[1,*], Edwin Mayes[2,*], Sharath Sriram[1]

[1]Functional Materials and Microsystems Research Group and the Micro Nano Research Facility, RMIT University, Melbourne, Australia
[2]RMIT Microscopy and Microanalysis Facility, RMIT University, Melbourne, Australia

*These authors contributed equally

Email Addresses of Co-authors:

Edwin Mayes (edwin.mayes@rmit.edu.au)

Corresponding Authors:

Shruti Nirantar (shruti.nirantar@gmail.com)
Sharath Sriram (sharath.sriram@rmit.edu.au)

KEYWORDS:

resistive switching, in situ transmission electron microscopy, crossbars, nanostructure analysis, volatile threshold switching, amorphous vanadium oxide

SUMMARY:

Presented here is a protocol for analyzing nanostructural changes during in situ biasing with transmission electron microscopy (TEM) for a stacked metal-insulator-metal structure. It has significant applications in resistive switching crossbars for the next generation of programmable logic circuits and neuromimicking hardware, to reveal their underlying operation mechanisms and practical applicability.

ABSTRACT:

Resistive switching crossbar architecture is highly desired in the field of digital memories due to low cost and high-density benefits. Different materials show variability in resistive switching properties due to the intrinsic nature of the material used, leading to discrepancies in the field because of underlying operation mechanisms. This highlights a need for a reliable technique to understand mechanisms using nanostructural observations. This protocol explains a detailed process and methodology of in situ nanostructural analysis as a result of electrical biasing using transmission electron microscopy (TEM). It provides visual and reliable evidence of underlying nanostructural changes in real time memory operations. Also included is the methodology of fabrication and electrical characterizations for asymmetric crossbar structures incorporating amorphous vanadium oxide. The protocol explained here for vanadium oxide films can be easily extended to any other materials in a metal-dielectric-metal sandwiched structure. Resistive switching crossbars are predicted to serve the programmable logic and neuromorphic circuits for

next-generation memory devices, given the understanding of the operation mechanisms. This protocol reveals the switching mechanism in a reliable, timely, and cost-effective way in any type of resistive switching materials, and thereby predicts the equipment's applicability.

INTRODUCTION:

Resistance change oxide memories are increasingly used as the building block for novel memory and logic architectures due to their compatible switching speed, smaller cell structure, and the ability to be designed in high capacity three-dimensional (3D) crossbar arrays[1]. To date, multiple switching types have been reported for resistive switching devices[2,3]. Common switching behaviors for metal oxides are unipolar, bipolar, complementary resistive switching, and volatile threshold switching. Adding on to the complexity, single cell has been reported to show multifunctional resistive switching performance as well[4-6].

This variability means that nanostructural investigations are needed to understand the origins of different memory behaviors and corresponding switching mechanisms to develop clearly defined condition-dependent switching for practical utility. Commonly reported techniques to understand the switching mechanisms are depth profiling with X-ray photoelectron spectroscopy (XPS)[7,8], nanoscale secondary ion mass spectroscopy (nano-SIMS)[6], nondestructive photoluminescence spectroscopy (PL)[8], electrical characterization of different size and thickness of functional oxide of devices, nanoindentation[7], transmission electron microscopy (TEM), energy-dispersive X-ray spectroscopy (EDX), and electron energy loss spectroscopy (EELS) on cross-sectional lamella in a TEM chamber[6,8]. All the above techniques have provided satisfactory insights about the switching mechanisms. However, in most of the techniques, more than one sample needs to be analyzed, including the original, electroformed, set, and reset devices, to understand the complete switching behavior. This increases experimental complexity and is time consuming. Additionally, the failure rates are high, because locating a subnanoscale filament in a device a few microns in size is tricky. Therefore, in situ experiments are important in nanostructural characterizations to understand operation mechanisms, as they provide evidence in real-time experiments.

Presented is a protocol for conducting in situ TEM with electrical biasing for metal-insulator-metal (MIM) stacks of asymmetric resistive switching cross-point devices. The primary goal of this protocol is to provide a detailed methodology for lamella preparation using a focus ion beam (FIB) and in situ experimental setup for TEM and electrical biasing. The process is explained using a representative study of asymmetric cross-point devices based on mixed-phased amorphous vanadium oxide (a-VO_x)[4]. Also presented is the fabrication process of cross-point devices incorporating *a*-VO_x, which can be easily scaled up to crossbars, using standard micro-nano fabrication processes. This fabrication process is important as it incorporates in crossbars *a*-VO_x which dissolves in water.

The advantage of this protocol is that with only one lamella, nanostructural changes can be observed in TEM, unlike the other techniques, where a minimum of three devices or lamellae are required. This significantly simplifies the process and reduces time, cost, and effort while providing reliable visual evidence of nanostructural changes in real-time operations. Additionally, it is designed with standard micro-nano fabrication processes, microscopy techniques, and instruments in innovative ways to establish its novelty and address the research gaps.

In the representative study described here for a-VO_x-based cross-point devices, the in situ TEM protocol helps to understand the switching mechanism behind apolar and volatile threshold switching[4]. The process and methodology developed for observing nanostructural changes in a-VO_x during in situ biasing can be easily extended to simultaneous analysis of the in situ temperature, temperature, and biasing, by just replacing the lamella mounting chip, and to any other material including two or more layers of functional material in a metal-insulator-metal sandwiched structure. It helps reveal the underlying operation mechanism and explain electrical or thermal characteristics.

PROTOCOL:

1. Fabrication process and electrical characterization

1.1. Use standard image reversal photolithography[9] to add the pattern with photoresist to the bottom electrode (BE) (layer 1) of the devices using the following parameters:

1.1.1. Spin coat the photoresist at 3,000 rpm, soft bake it at 90 °C for 60 s, expose with 25 mJ/cm^2 with a 405 nm laser, bake at 120 °C for 120 s, perform flood exposure with 21 mW/cm^2 and a 400 nm laser, develop using developer, and rinse with deionized water.

1.2. Deposit 5 nm titanium (Ti) for adhesion and 15 nm of platinum (Pt) on top with an electron beam evaporator system on the substrate patterned on layer 1.

1.3. Lift-off the deposited metals by placing the substrate in an acetone bath for ~20 mins. Then, apply ultrasonic vibrations for 2 min, and rinse with acetone and isopropyl alcohol (IPA) to complete the BE patterns. Repeat if the lift-off is not clean (**Figure 1A, step 1**).

1.4. Pattern the functional oxide layer (layer 2) with photolithography on top of the BE as described in step 1.1.

1.5. Deposit ~100 nm of a-VO_x and 5 nm of Ti on top of layer 2 using a sputtering system[10].

1.6. Lift-off the functional oxide by placing the substrate in an acetone bath and applying pulsed ultrasonic vibrations manually with 2–3 s pulses to finalize the functional oxide patterns. Repeat the procedure if the patterns are not clean. (**Figure 1A, step 2 and step 3**)

1.7. Similarly, complete the top electrode (TE) (layer 3) patterns with Ti_20 nm/Pt_200 nm using image reversal photolithography, electron beam evaporation, and the lift-off process described in steps 1.1, 1.2, and 1.3. (**Figure 1A, step 4**)

NOTE: This completes the fabrication of the cross-point device, **Figure 1B**.

1.8. Perform electrical and temperature analysis on the fabricated device to understand its resistance switching performance.

1.8.1. Use the source meter with two-probe direct current (DC) *I–V* measurement system and a probe station for electrical measurements.

1.8.2. Always maintain the relevant current compliance to avoid damaging the devices.

1.8.3. To analyze the device's current behavior, perform voltage-controlled analysis and apply voltage sweeps starting with a low voltage of 0.1 V in positive bias and increasing slowly until electroforming is observed.

NOTE: Electroforming is a one-time event at which a few nanometer-wide conductive filaments are formed within the initially insulating functional oxide at a particular voltage, which depends on intrinsic material properties and device dimensions. At this point, a sudden drop in resistance or increase in current is observed on the current-voltage graph due to a formed conductive path.

1.8.4. After electroforming, apply bidirectional voltage sweeps to achieve volatile threshold switching performance. Adjust the voltage to achieve a high ON/OFF ratio. In this case, a switching ratio of ~10 was attained.

1.8.5. Analyze the current-voltage characteristics at different temperatures from room temperature to 90 °C increasing in 10 °C steps and reverse back to room temperature using a temperature-controlled stage.

2. Gridbar and biasing chip mounting

2.1. Design the FIB optimized gridbar in CAD software and manufacture using standard machining techniques in-house for mounting the biasing/heating chips used for in situ TEM experiments, as shown in **Figure 2**.

NOTE: **Figure 2A** shows separate parts of the gridbar to mount three chips simultaneously in the square shaped trenches. **Figure 2B** shows the zoomed squared trench section designed to fit the commercially available in situ biasing/heating chips for TEM.

2.2. Clean the biasing chip by placing it in a glass Petri dish filled with acetone and gently rotate for 2 min. Then remove the chip and place it in a Petri dish filled with methanol and gently rotate for 2 min. Finally, blow dry with low pressured nitrogen.

NOTE: Commercially bought biasing chips, referred to as E-chips, have a photoresist coating for protection.

2.3. Align the precleaned biasing chip in square trenches of gridbar, as seen in **Figure 2C**.

2.4. Fix the grid cover on top of the biasing chip with screws to finalize the placement of the E-chip on the gridbar (**Figure 2D**).

3. Lamella preparation, mounting on biasing chip using focused ion beam, and in situ transmission electron microscopy

3.1. Fabricate the samples separately as described in section 1 with a thicker BE of Ti_10 nm/Pt_100 nm, as seen in **Figure 3A**.

3.2. Mount the newly prepared sample on a metal stub using conductive carbon tape and load in the FIB chamber. Apply additional tape on the sample for grounding to avoid charging problems.

3.3. Load the biasing chip-mounted gridbar in the chamber at a 52° tilt (see **Figure 3B**). This will be either perpendicular or parallel to the ion beam column depending on the stage rotation.

3.4. Focus, astigmate, and align the electron beam on a sample surface using the microscope physical control panel and software on lamella preparation locations.

3.5. Check the eucentric height of the focused sample location and beam coincidence for the electron beam and ion beam.

NOTE: The eucentric height is the position where the sample's image does not move when the sample is tilted.

3.6. Click on **Auto TEM program** (automatic lamella preparation program) to run it on the focused sample location using the microscope control software. The automatic program follows the sequence described below.

NOTE: This will complete the process for creating a TEM lamella (**Figure 4**). The progress of the AutoTEM program can be observed live on the desktop screen.

3.6.1. Create cross fiducial alignment markers with silicone milling and deposit a 1.5 µm-thick carbon protective layer over the 20 µm x 5 µm area between alignment markers.

3.6.2. Mill trenches on either side of carbon protective layer with a 5 nA ion beam current to create the lamella.

3.6.3. Thin the lamella with a 1 nA ion beam current first and then with 300 pA ion beam current to reach a 1 µm thickness.

3.7. Tilt the sample to 7° to perform a J-cut on the lamella for separation from the substrate.

3.8. Tilt the sample to 0° (i.e., perpendicular to the electron beam column) and attach the lamella to the manipulator needle by wielding using Pt (**Figure 5A**).

3.9. After attachment to the micromanipulator, separate the lamella from the substrate with the final cut and slowly retract the micromanipulator (**Figure 5B**).

3.10. Focus the beam on the top edge of biasing chip on the gridbar, the lamella mounting position.

3.11. Bring the lamella slowly towards the biasing chip with the manipulator needle (**Figure 6A**).

3.12. Align the lamella in the center of the 17 µm gap on the top edge of the biasing chip. Slowly move it down until it barely touches the chip surface and weld the bottom edges of the lamella to the chip using Pt (**Figure 6B**).

3.13. Cut the micromanipulator free from the lamella with silicon milling and retract the micromanipulator.

3.14. Connect the top edges of the lamella with Pt traces to the two electrodes of the biasing chip for electrical connections (**Figure 6C**).

NOTE: The TE and BE are shorted at this point on both left and right sides.

3.15. Thin the center region of lamella first using 300 pA, and then with 100 pA ion beams to make the lamella less than 100 nm thick (**Figure 6D**) by tilting the specimen front and back by 2° to ensure parallel faces and a uniform thickness.

3.16. Polish out the ion beam-damaged layer with the Ga beam accelerating voltage of 5 kV at an angle of 5° to the surface on both faces.

3.17. Remove the short connection between the top and bottom electrodes of the device with isolation cuts in the thinned region to create a current path from BE to TE through the active region (**Figure 7A**).

3.18. Mount the biasing chip with lamella on the biasing chip holder and then load the biasing chip holder into the TEM chamber.

3.19. Connect the wires from the biasing chip holder to the source meter and a control PC.

NOTE: Carefully place the connection wires to relieve the strain and minimize any vibrations during the experiment.

3.20. Wait for the TEM chamber pressure to drop to 4e-5 Torr and then focus, astigmate, and align the electron beam on a cross section of the lamella surface using the TEM control knobs.

3.21. Apply voltage sweeps or constant voltage at different biasing voltages and collect the TEM micrographs in situ.

NOTE: Data related to diffraction patterns, electron diffraction X-ray spectroscopy (EDX), and electron energy loss spectroscopy (EELS) mapping can also be collected at different biasing voltages in situ.

REPRESENTATIVE RESULTS:

The results achieved using this protocol for the *a*-VO_x cross-point devices are explained in **Figure 8**. **Figure 8A** shows the TEM micrograph of the intact lamella. Here the diffraction patterns (inset) indicate the amorphous nature of the oxide film. For the in situ measurements, TEM-controlled voltages were applied starting from 25 mV to 8 V in 20 mV steps with the bottom electrode (BE) positively biased and top electrode (TE) grounded. **Figure 8B** shows that at 4 V a localized crystalline region formed in the oxide layer. Here, *d*-spacing was 0.35 nm, as shown in the high-resolution TEM (HRTEM) and diffraction patterns (insets). This *d*-spacing corresponds to the (011) plane of the VO_2–M1 phase[10,11]. **Figure 8C** shows the multiple localized crystal islands within the oxide layer at 5 V. These crystal islands were oriented in different directions with respect to the substrate. Two different *d*-spacings can be observed in the corresponding FFT and HRTEM (insets): 0.35 nm and 0.27 nm. A spacing of 0.27 nm corresponds to the VO_2–A phase, while 0.26 nm corresponds to the VO_2–M1 phase[12]. Considering the aberration defects and tilt correction limits of the instrument, the observed 0.27 nm *d*-spacing likely corresponds to the mixed phase of VO_2–M1 and VO_2–A. **Figure 8D** shows the Moiré fringes at 6 V. There are multiple nucleation sites in the lamella. Here FFT and HRTEM (insets) provide further evidence of the different orientations of the VO_2–M1 crystal islands. After 6 V, the lamella is completely crystallized with multiple orientations only with the electrical bias without any conventional annealing.

This is the first demonstration of *a*-VO_x thin film crystallizing into localized *c*-VO_2 islands with electric bias. The strong evidence for the presence of *c*-VO_2 islands in *a*-VO_x devices after biasing at higher voltage proves the resistive switching characteristics (Figure 2 of cited reference[4]) and the switching mechanism (Figure 6 of the cited reference[4]) for asymmetric cross-point devices based on mixed-phased *a*-VO_x.

The results show the application of the explained protocol. Here the in situ nanostructural changes were captured in remanence of voltage sweeps at different voltages with the high-resolution TEM (HRTEM) micrographs and corresponding diffraction patterns.

FIGURE AND TABLE LEGENDS:

Figure 1: Fabrication flow and cross-point device structure schematic. (**A**) Fabrication flow incorporating Ti capping to protect *a*-VO_x film from dissolving in water. (**B**) Schematic of cross-point device structure. This figure has been modified from Nirantar et al.[4].

Figure 2: Custom-made FIB optimized gridbar for in situ mounting of TEM chips. (**A**) Individual

parts of the gridbar. (**B**) Squared trench for in situ TEM chip placement. (**C**) Aligned biasing chip for in situ TEM in the squared trench. (**D**) Mounted biasing chip on the gridbar.

Figure 3: Cross section stacks for in situ samples and FIB chamber setup of biasing chip. (**A**) Cross section stacks of devices prepared separately for in situ biasing using TEM sample. (**B**) Gridbar setup in the chamber to allow access to the scanning electron microscopy (STEM) detector for precision cutting and connections on the lamella.

Figure 4: Processing steps of Auto TEM. (**A**) Alignment markers and protection layer deposition. (**B**) Trenches formed with rough milling using a 5 nA current.

Figure 5: The process of lamella separation from the substrate. (**A**) Manually made J-cut and attached lamella to the manipulator needle. (**B**) Extracted lamella through the trenches after the final separation cut.

Figure 6: Lamella mounting on the biasing chip process. (**A**) Manipulator bringing the attached lamella to the biasing chip. (**B**) Lamella attached to the biasing chip. (**C**) Connections with platinum traces between the electrodes of the biasing chip and the region of interest of the lamella. (**D**) Sub-100 nm thinned center region of the lamella.

Figure 7: Final isolation cuts and the current path in the lamella and micrograph of the FIB optimized biasing chip.

Figure 8: In situ electrical transmission electron microscopy. (**A**) Original lamella. The inset shows the FFT of the functional layer. (**B**) Micrograph after 4 V biasing. FFT inset shows c-VO_2 (M1) phase with (011) plane and HRTEM inset shows the fringes separation as 0.35 nm. (**C**) Micrograph after 5 V. FFT and HRTEM insets show multiple nucleation sites and different orientations of the same c-VO_2–M1. (**D**) Micrograph after 6 V. FFT inset shows different orientations of same c-VO_2 – M1 phase. HRTEM inset shows the formation of Moiré fringes. This figure has been modified from Nirantar et al.[4].

DISCUSSION:

This paper explains the protocol for in situ biasing with transmission electron microscopy including the fabrication process for the device, gridbar designing for biasing chip mounting, lamella preparation and mounting on the biasing chip, and TEM with in situ biasing.

The fabrication methodology of cross-point devices, which can be easily scaled up to crossbar structures, is explained. The Ti capping of vanadium oxide is essential to incorporate amorphous vanadium oxide, because it dissolves in water during the fabrication steps after a-VO_x deposition. Devices are fabricated with two different sizes for electrical testing, 4 µm x 4 µm and 6 µm x 6 µm. The contact electrode used here is Pt, a noble metal that degrades minimally over the fabrication period. Due to this and to avoid the uniform crystallization of vanadium oxide in the device structure, the electrode annealing step typically used was omitted in this fabrication method. A complete fabrication flow and the device structure schematic is presented **Figure 1**[4].

For in situ experiments, the devices are fabricated separately with thicker BE as explained in step 1 of the lamella preparation and mounting on biasing chip section. This is done to avoid the deposition of Pt particles on the functional layer during connections. The change in thickness of the BE is not expected to have an effect in device switching.

The commercially available biasing chips (e.g., E-chip) for in situ biasing with TEM have four biasing electrodes available for connection and a 17 µm wide gap for mounting the lamella, as shown in **Figure 7B**. A customized gridbar is designed to mount the biasing chips, as this arrangement allows access to the scanning transmission electron microscopy (STEM) detector in the FIB chamber for precise cutting and connection of the lamella mounted on the biasing chip. This is especially required for the precise isolation cuts explained in step 17 of the lamella preparation and mounting on the biasing chip section. For the lamella preparation and mounting process, the sequence of Pt connections, lamella thinning, and making isolation cuts (steps 14–17 of lamella preparation and mounting) are the most critical to achieve a clean lamella. Here, the Pt connecting traces are performed before the thinning process to avoid deposition of Pt particles on the functional oxide layer, which can ruin electrical attributes.

Because the lamella is prepared using Ga ion milling, some undesirable Ga contamination is expected in the final lamella. However, lamella polishing is performed to significantly reduce the damage caused by the Ga beam. Another drawback of this protocol is that the dimensions of the lamella are significantly smaller (in nanoscale) compared to the actual device (a few microns). Due to this, variability can be observed in the electrical characterizations of the actual device and the lamella-based device.

Despite of that, this protocol offers a significant advantage over the existing techniques, because it provides visual verification of every step of the lamella preparation and during the in situ biasing. As all the steps can be seen visually in real time, failures are detected and rectified immediately. There are no hidden aspects in the process and troubleshooting is simply by visual observation unless there are any instrument specific issues.

The presented methodology has a notable impact in the field of material science and resistive switching devices compatible with high vacuum conditions. The protocol can explain the electrical results and operation mechanisms based on visually observed nanostructural changes in situ. This protocol will influence next generation of nanoelectronics, logic circuits, neuromorphic devices, and material sciences to reveal the underlying operation mechanisms and predict the practical applicability of novel structures and materials.

ACKNOWLEDGMENTS:
This work was performed in part at the Micro Nano Research Facility at RMIT University in the Victorian Node of the Australian National Fabrication Facility (ANFF). The authors acknowledge the facilities, and the scientific and technical assistance of the RMIT University's Microscopy, Microanalysis Facility, a linked laboratory of the Microscopy Australia. Scholarship support from the Australian Postgraduate Award (APA)/Research Training Program (RTP) scheme of the

Australian government is acknowledged. We thank Professor Madhu Bhaskaran, Associate Professor Sumeet Walia, Dr. Matthew Field, and Mr. Brenton Cook for their guidance and helpful discussions.

DISCLOSURES:

The authors have nothing to disclose.

REFERENCES:

1. Kozma, R., Pino, R. E., Pazienza, G. E. in *Advances in Neuromorphic Memristor Science and Applications*. eds. Robert Kozma, Robinson E. Pino, Giovanni E. Pazienza. Springer Netherlands. pp. 9–14 (2012).

2. Pan, F., Gao, S., Chen, C., Song, C., Zeng, F. Recent progress in resistive random access memories: Materials, switching mechanisms, and performance. *Materials Science and Engineering: R: Reports.* **83**, 1–59 (2014).

3. Zhou, Y., Ramanathan, S. Mott Memory and Neuromorphic Devices. *Proceedings of the IEEE.* **103** (8), 1289–1310 (2015).

4. Nirantar, S. et al. In Situ Nanostructural Analysis of Volatile Threshold Switching and Non-Volatile Bipolar Resistive Switching in Mixed-Phased a-VOx Asymmetric Crossbars. *Advanced Electronic Materials.* **5** (12), 1900605(2019).

5. Rupp, J. A. et al. Different threshold and bipolar resistive switching mechanisms in reactively sputtered amorphous undoped and Cr-doped vanadium oxide thin films. *Journal of Applied Physics.* **123** (4), 044502 (2018).

6. Ahmed, T. et al. Inducing tunable switching behavior in a single memristor. *Applied Materials Today.* **11**, 280–290 (2018).

7. Nili, H. et al. Nanoscale Resistive Switching in Amorphous Perovskite Oxide (a-SrTiO3) Memristors. *Advanced Functional Materials.* **24** (43), 6741–6750 (2014).

8. Ahmed, T. et al. Transparent amorphous strontium titanate resistive memories with transient photo-response. *Nanoscale.* **9** (38), 14690–14702 (2017).

9. Reuhman-Huisken, M. E., Vollenbroek, F. A. An optimized image reversal process for half-micron lithography. *Microelectronic Engineering.* **11** (1), 575–580 (1990).

10. Taha, M. et al. Insulator–metal transition in substrate-independent VO2 thin film for phase-change devices. *Scientific Reports.* **7** (1), 17899 (2017).

11. Booth, J. M. et al. Correlating the Energetics and Atomic Motions of the Metal-Insulator Transition of M1 Vanadium Dioxide. *Scientific Reports.* **6**, 26391 (2016).

12. Lee, S., Ivanov, I. N., Keum, J. K., Lee, H. N. Epitaxial stabilization and phase instability of VO2 polymorphs. *Scientific Reports.* **6**, 19621 (2016).

Figure 1 Click here to access/download;Figure;Figure 1.png

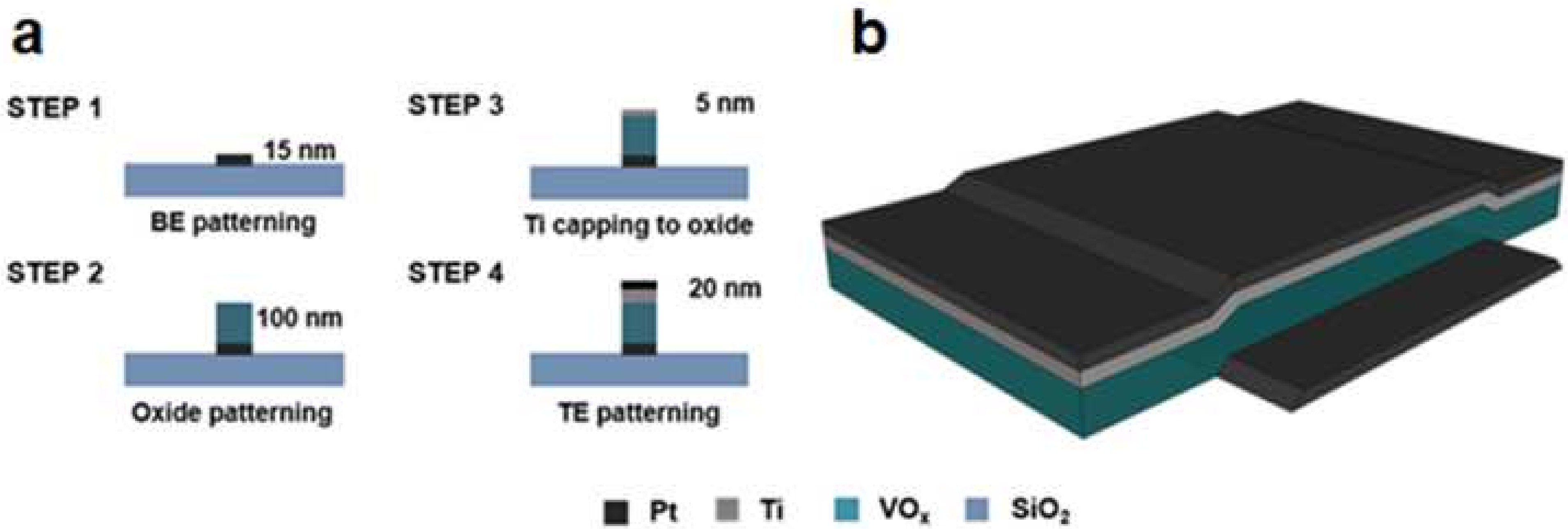

Figure 2

Click here to access/download;Figure;Figure 2.png

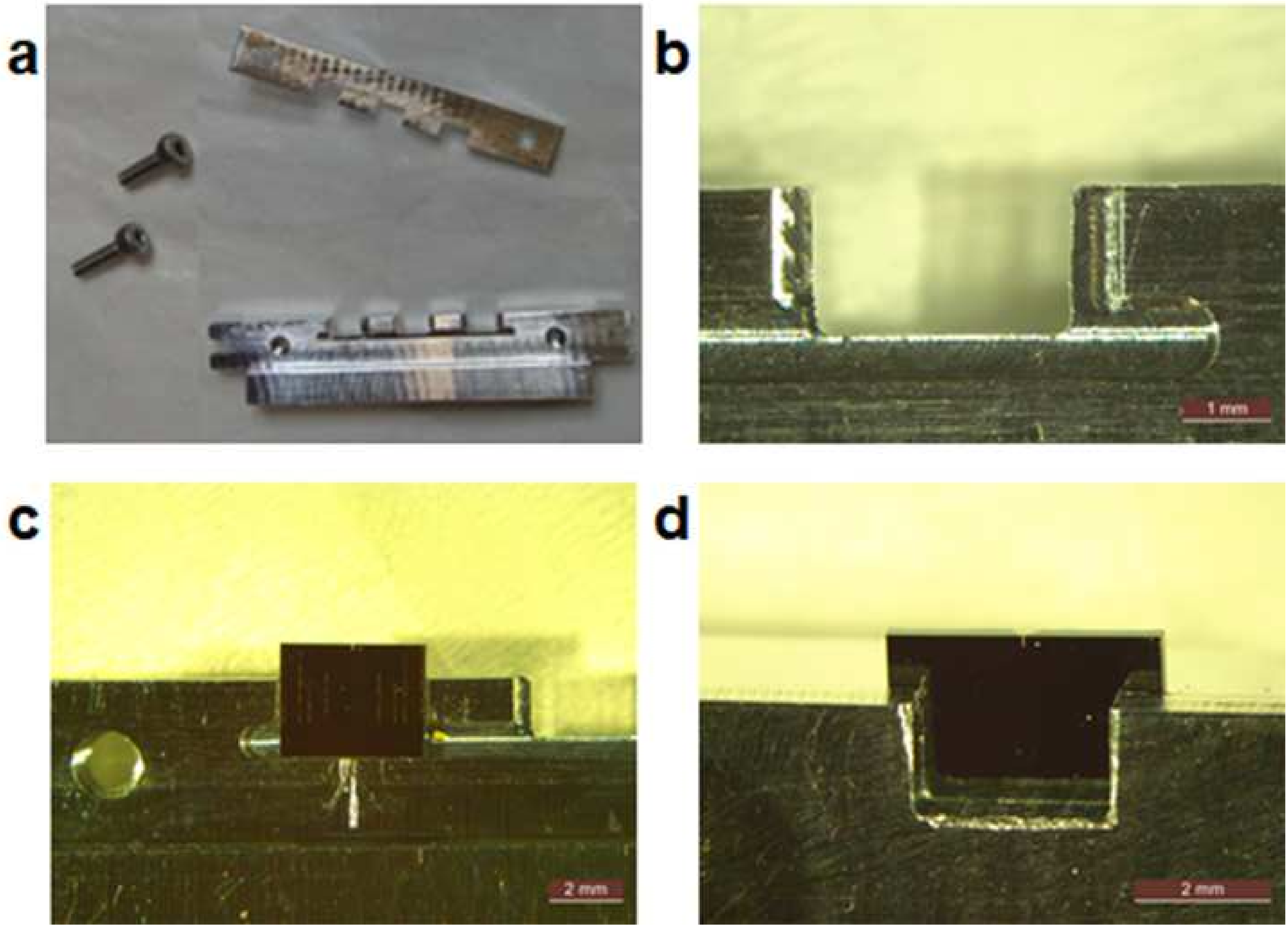

Figure 3

Click here to access/download;Figure;Figure 3.png

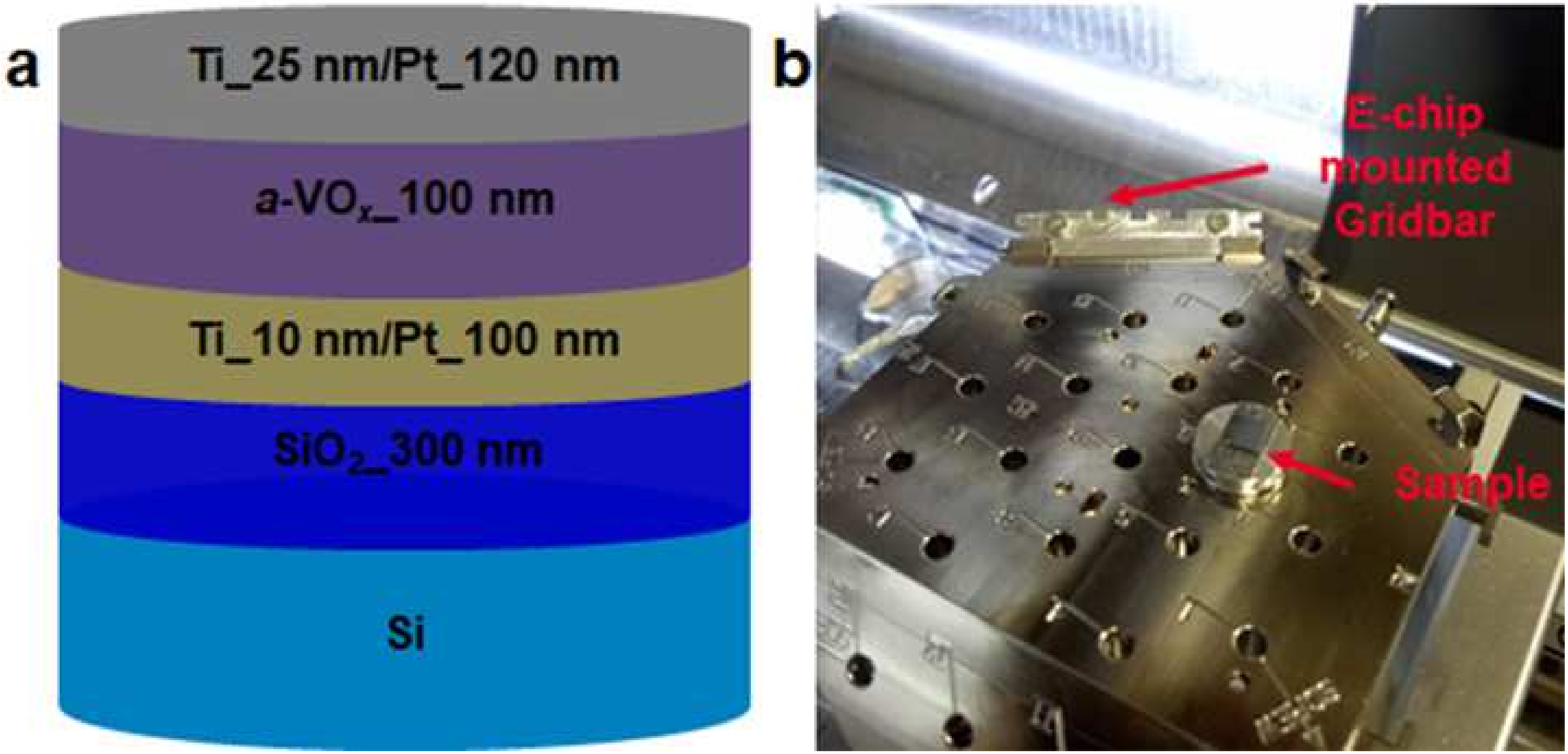

Figure 4

Click here to access/download;Figure;Figure 4.png

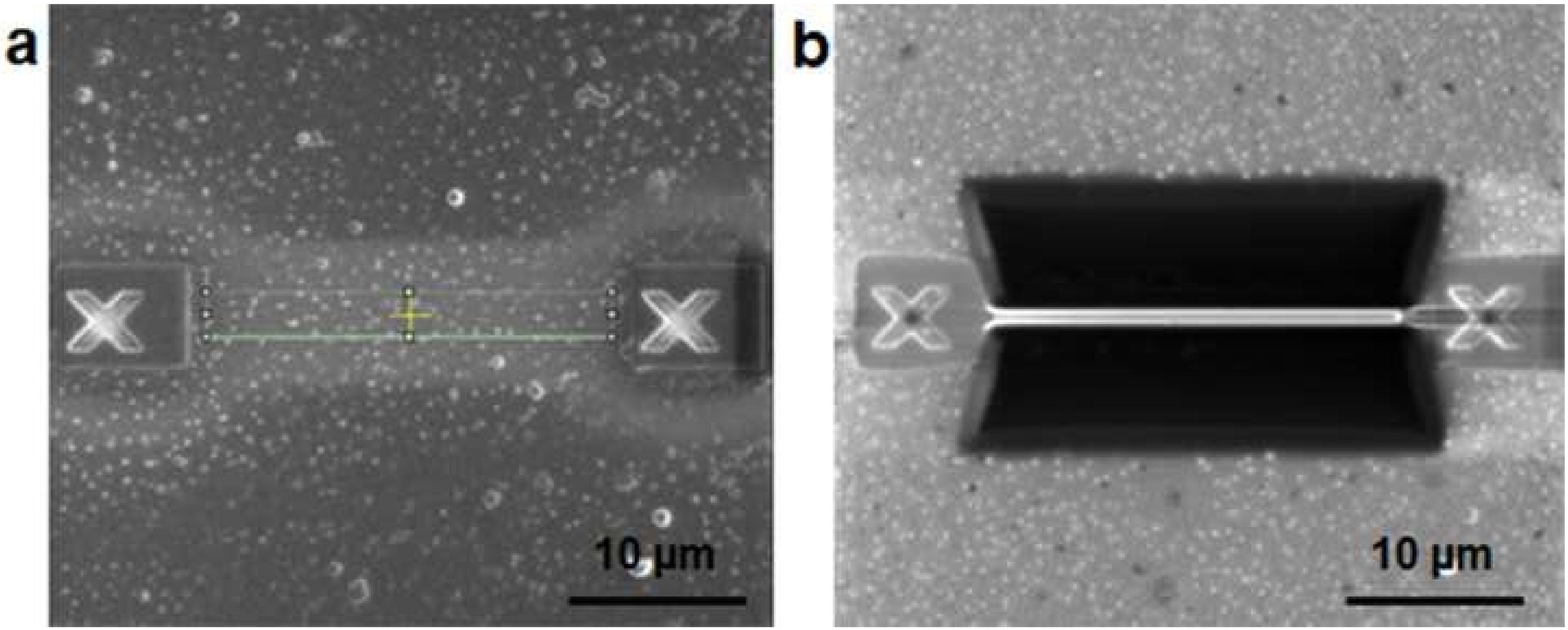

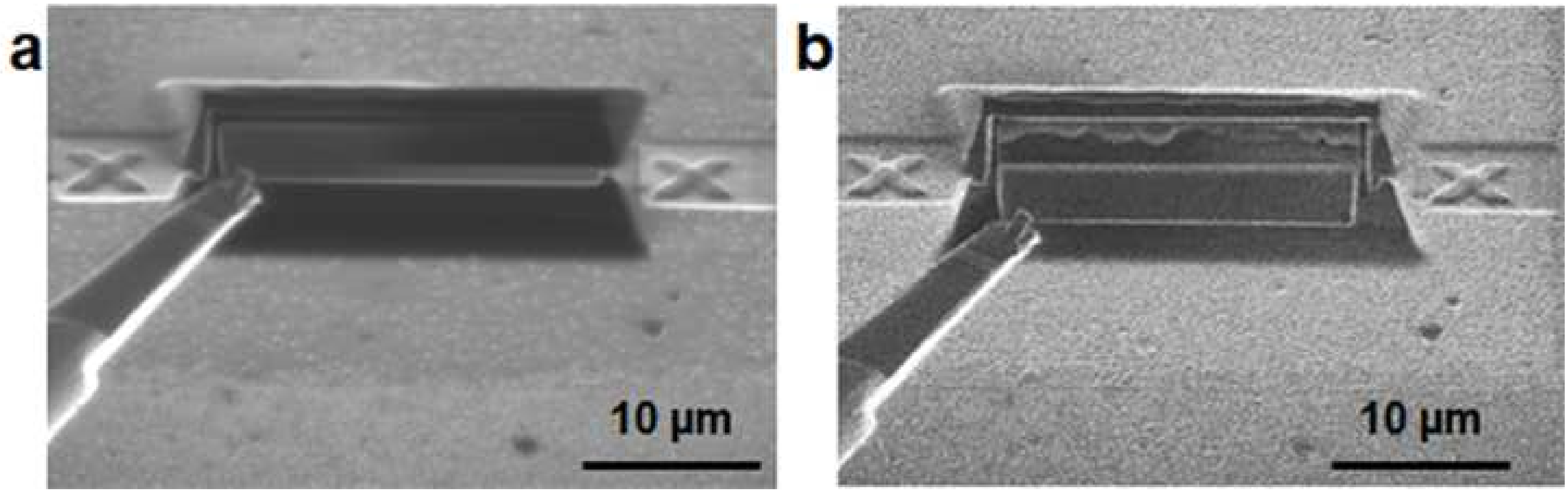
a
10 µm
b
10 µm

Figure 6

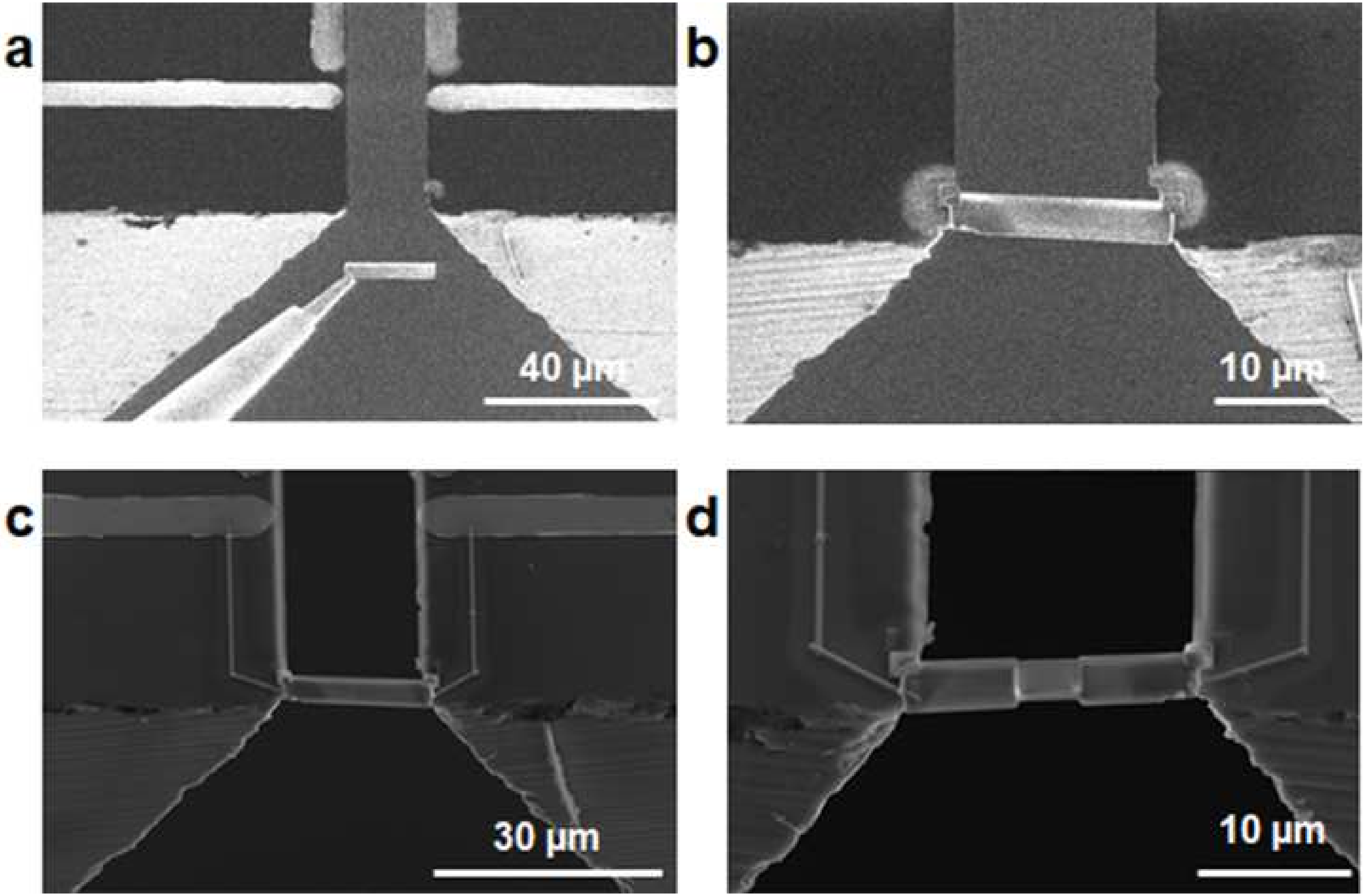

Figure 7

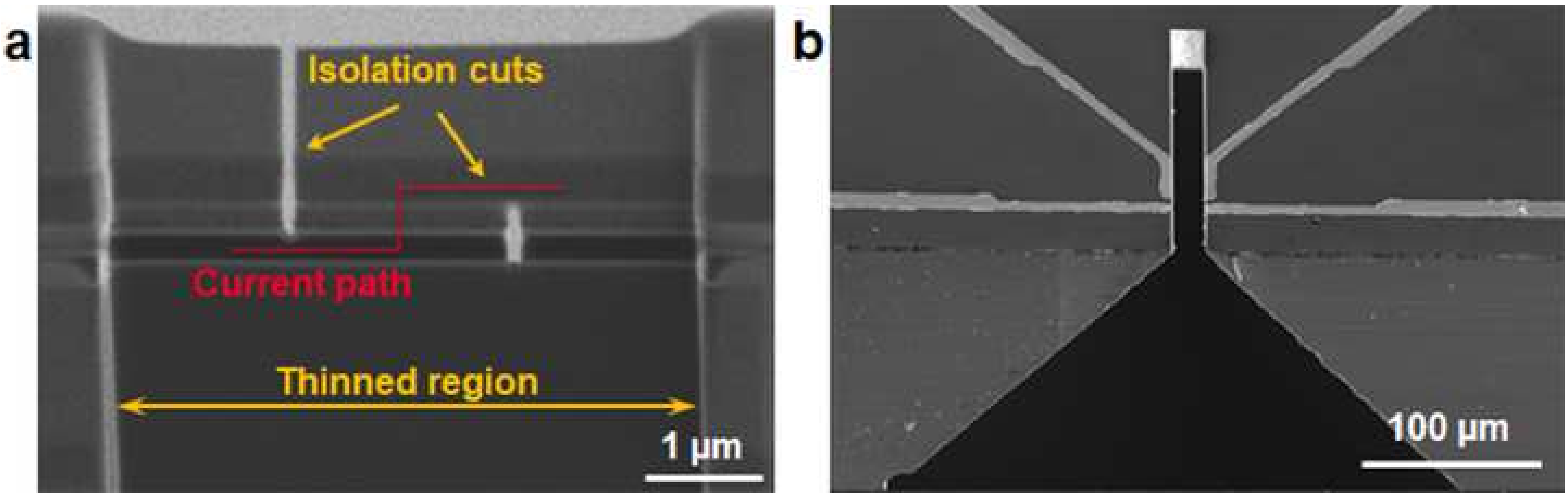

Figure 8

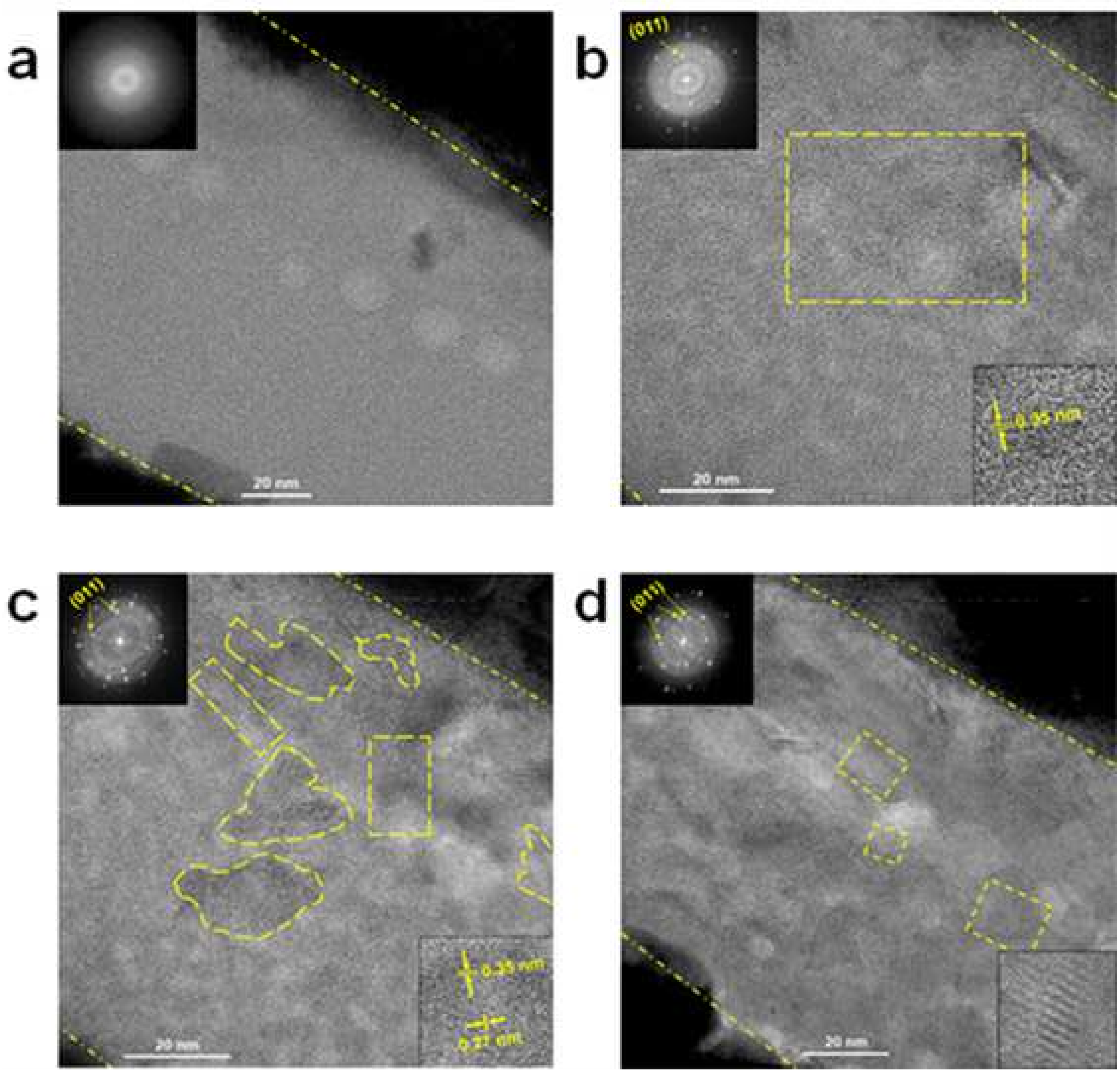

Name of Material/ Equipment	Company	Catalog Number
Resist processing system	EV group	EVG 101
Acetone	Chem-Supply	AA008
Biasing Chip - E-chip	Protochips	E-FEF01-A4
Developer	MMRC	AZ 400K
Electron beam evaporator - PVD 75	Kurt J Leskar	PRO Line - eKLipse
Focused Ion beam system	Thermo Fisher - FEI	Scios DualBeam^{TM} system
Hot plates	Brewer Science Inc.	1300X
Magnetron Sputterer	Kurt J Leskar	PRO Line
Mask aligner	Karl Suss	MA6
Maskless Aligner	Heildberg instruments	MLA150
Methanol	Fisher scientific	M/4056
Phototresist	MMRC	AZ 5412E
Pt source for e-beam evaporator	Unicore	
The Fusion E-chip holder	Protochips	Fusion 350
Ti source for e-beam evaporator	Unicore	
Transmission Electron Microscope	JEOL	JEM 2100F

Comments/Description

Manuscript ID	**:**	JoVE61026
Title	**:**	Fabrication process and *in situ* nanostructural analysis methodology of volatile threshold switching in mixed-phased a-VOx based asymmetric crossbars

RESPONSE TO THE REVIEWERS

Authors thanks the Editor and Reviewers for their time and constructive comments. We believe that the feedback has resulted in significant improvements in quality of the manuscript. We have revised our manuscript in line with all comments and suggestions made. We have also included additional references, discussions and clarifications. The modified and additional text in manuscript is marked in red.

Editorial comments:

Comment 1

Please take this opportunity to thoroughly proofread the manuscript to ensure that there are no spelling or grammar issues. The JoVE editor will not copy-edit your manuscript and any errors in the submitted revision may be present in the published version. Please use American English throughout.

Response

Manuscript has been updated and proofread thoroughly.

Comment 2

Please format the manuscript as: paragraph Indentation: 0 for both left and right and special: none, Line spacing: single. Please include a single line space between each step, substep and note in the protocol section. Please use Calibri 12 points.

Response

Manuscript updated as per JoVE template. All the above mentioned changes are included.

Comment 3

Please provide an email address for each author.

Response

Email address of all the authors are provided in affiliation section on lines 15-20.

Comment 4

Please rephrase the Short Abstract/Summary to clearly describe the protocol and its applications in complete sentences between 10-50 words: "Here, we present a protocol to …"

Response

The short abstract has been rephrased and updated on lines 27-31.

Comment 5

Please ensure that the long Abstract is within 150-300-word limit and clearly states the goal of the protocol.

Response

The long abstract has been revised as per the requirements on lines 35-50.

Comment 6

Unfortunately, there are a few sections of the manuscript that show significant overlap with previously published work. Though there may be a limited number of ways to describe a technique, please use original language throughout the manuscript. Please see lines: 36-39, 45-46, 54-56, 102-105, 110-113, 116-119, 246-264, 273-275.

Response

All the above sections have been revised to avoid the overlap to the best of our ability. However, there might be some overlap in representative results corresponding figure captions, which is unavoidable. With copyright permissions and appropriate citation, we believe it should be acceptable as has been communicated before.

For line 273-275, the overlap is for the facility acknowledgement. This cannot be rewritten or removed.

Comment 7

JoVE cannot publish manuscripts containing commercial language. Please remove all commercial language from your manuscript and use generic terms instead. All commercial products should be sufficiently referenced in the Table of Materials and Reagents. For example: AZ5214E photoresist, MLA150 Maskless Aligner – Heildberg

instruments, Lesker PVD75, Keithley 4200 source-meter, Linkam, JEOL 2100F, FEI Scios DualBeamTM system, Protochips, E-chips, Fusion biasing holder, etc.

Response

All the commercial language is removed from the main manuscript and all commercial products are reference in the Table of Materials and Reagents.

Comment 8

Please revise the Introduction to include all of the following with citations:

a) A clear statement of the overall goal of this method

b) The rationale behind the development and/or use of this technique

c) The advantages over alternative techniques with applicable references to previous studies

d) A description of the context of the technique in the wider body of literature

e) Information to help readers to determine whether the method is appropriate for their application

Response

The introduction section is revised to include all the above suggested points on line 51 to 95.

Comment 9.

The Protocol should contain only action items that direct the reader to do something in a stepwise manner. Please move the discussion about the protocol to the Discussion.

Comments 10

The Protocol should be made up almost entirely of discrete steps without large paragraphs of text between sections. Please ensure that individual steps of the protocol should only contain 2-3 actions per step.

Comment 11

Please make sections in the protocol to help navigate from one step to the next.

Comment 12

Please adjust the numbering of the Protocol to follow the JoVE Instructions for Authors. For example, 1 should be followed by 1.1 and then 1.1.1 and 1.1.2 if necessary. Please refrain from using bullets or dashes.

Comment 13

Please ensure that all text in the protocol section is written in the imperative tense as if telling someone how to do the technique (e.g., "Do this," "Ensure that," etc.). The actions

should be described in the imperative tense in complete sentences wherever possible. Avoid usage of phrases such as "could be," "should be," and "would be" throughout the Protocol. Any text that cannot be written in the imperative tense may be added as a "Note."

Comment 14

Please add more details to your protocol steps. Please ensure you answer the "how" question, i.e., how is the step performed? Please include discrete experimental steps, button clicks in the software, knob turns in the instruments etc.

<u>Response</u>

The protocol has been updated to incorporate all the comments from 9 to 14 on lines 97 to 208.

Comment 15

What kind of image was used for the study? Reference for standard image? How was the patterning performed? How was the deposition performed, what are the conditions used? How do you liftoff the patterns?

<u>Response</u>

We believe that the editor is referring to the fabrication process here. A standard and well known image reversal photolithography recipe was used for patterning. "Image reversal" is name of the process. The masks used for photolithography replicate the device schematic presented in Figure 10. All the details about patterning, deposition, and lift-off are included in the protocol on lines 98 to 118.

Please note that all the steps in device fabrication section, from the methodology point of view are standard. There are seven instruments used in this process. If we include all the minor details of how those 7 instruments were used in this fabrication, it will be more than 10 pages. While that is not the core idea of this paper, every lab has different set of instruments to perform standard processes and in depth explanation on how that action was performed will not be widely useful.

We have revised this section and included all the critical steps, conditions, and parameters sufficient to replicate the fabrication.

Comment 16

How was the electrical charactezation performed? Please describe the actions associated with it. What are the parameters being studied and how?

<u>Response</u>

We have revised this section and details are explained on lines 119 -130.

Comment 17

Lines 101-108, 110-114, 116-120, 159-160, 162-173, 178-184, 189-192, 241-242: Either make action steps or move to the intro/results/discussion wherever applicable.

Response

The updates have been included as requested. Now the protocol includes only action steps, rest of the details have been moved to discussion section.

Comment 18

Line 122: How were the samples prepared for in situ biasing experiments, condition etc?

Response

We believe the Editor is referring to the fabrication of the sample which is separately prepared for *in situ* experiment. The sample which is fabricated separately follows the same procedure as explained in fabrication procedure section on lines 98-118, with one modification which is explained on lines 150-153.

The lamella preparation and mounting on biasing chip section of the protocol explains the procedure for *in situ* lamella preparation on lines 150-153.

Comment 19

Line 143: What is the set up for Auto TEM program.

Auto TEM setup explained on lines 163-171.

Comment 20

Line 144: How is this done?

Response

The details are provided in gridbar and biasing chip mounting section on lines131-148.

Comment 21

Step 6: how was this done? Please describe all the actions.

Response

It has been explained with a note in the lamella preparation and mounting on biasing chip section on lines 197-198.

Please note that these actions are the basic operations of any electron microscope for pre-processing adjustments. The specific actions such as use of software, mouse or keyboard will change with the instrument and software. The focus of this protocol is not the preliminary focusing, astigmatism or beam alignment of focused ion beam (FIB) used in this case. The same experiment can be performed with other FIB. To target the larger audience, we believe it would be beneficial to provide critical details and conditions sufficient to replicate the experiment.

Comments 22

There is a 10-page limit for the Protocol, but there is a 2.75-page limit for filmable content. Please highlight 2.75 pages or less of the Protocol (including headings and spacing) that identifies the essential steps of the protocol for the video, i.e., the steps that should be visualized to tell the most cohesive story of the Protocol.

Response

The main protocol is highlighted in Grey color.

Comments 23

Please do not combine the results and discussion section. Please include at least one paragraph of text to explain the Representative Results in the context of the technique you have described, e.g., how do these results show the technique, suggestions about how to analyze the outcome, etc. The paragraph text should refer to all of the figures. Data from both successful and sub-optimal experiments can be included.

Response

A separate section for representative results is included in the revised manuscript on lines 210 to 237. The context of the representative results section has been revised to include all the comments from Editors.

Comment 24

Please discuss all figures in the Representative Results. However, for figures showing the experimental set-up, please reference them in the Protocol.

Response

All the Figures relevant to the representative results section (Figure 7) are discussed there. The image relating to fabrication flow and device schematics (Figure 8) is discussed in discussion section. Rest all the figures show experimental set-up and are addressed in the protocol.

Comment 25

Please include all the Figure Legends together at the end of the Representative Results in the manuscript text. Each Figure Legend should include a title and a short description of the data presented in the Figure and relevant symbols. The Discussion of the Figures should be placed in the Representative Results. Details of the methodology should not be in the Figure Legends, but rather the Protocol.

Response

The figure captions are placed after representative results section in the suggested format.

Comment 26

Please obtain explicit copyright permission to reuse any figures from a previous publication. Explicit permission can be expressed in the form of a letter from the editor or a link to the editorial policy that allows re-prints. Please upload this information as a .doc or .docx file to your Editorial Manager account. The Figure must be cited appropriately in the Figure Legend, i.e. "This figure has been modified from [citation]."

Response

The copyright permissions are obtained and are submitted along with the revision. All the relevant figures and text has been cited appropriately.

Comment 27

As we are a methods journal, please revise the Discussion to explicitly cover the following in detail in 3-6 paragraphs with citations:

a) Critical steps within the protocol

b) Any modifications and troubleshooting of the technique

c) Any limitations of the technique

d) The significance with respect to existing methods

e) Any future applications of the technique

Response

The discussion section has been updated to include all the above suggested points on lines 277–320.

Comment 28

We do not have a separate conclusion section. Please merge it with the discussion section instead.

Response

The conclusion section is removed and merged with discussion section.

Comment 29

Please remove the embedded figure(s) from the manuscript. All figures should be uploaded separately to your Editorial Manager account. Each figure must be accompanied by a title and a description after the Representative Results of the manuscript text. All panels of one figure should be combined. Please do not put the legends along with the figures.

Response

A separate file for figures is created, captions are updated to have a title and short description. The revised manuscript is updated as per the above instructions.

Comment 30

Please revise the table of the essential supplies, reagents, and equipment. The table should include the name, company, and catalog number of all relevant materials in separate columns in an xls/xlsx file.

Response

The table of the essential supplies, reagents, and equipment is revised as per the instructions.

Reviewer 1

Comment 1

In Fig1a step 4, the top Ti and Pt has a larger lateral area than VOx, while in Fig. 1b they are of the same size. The authors need to make them consistent.

Response

We thank the Reviewer for bring it to our attention. The fabrication flow Fig 1a has been modified to match the device schematic

Modification

In Figures document

Modified section in highlighted in red boundary.

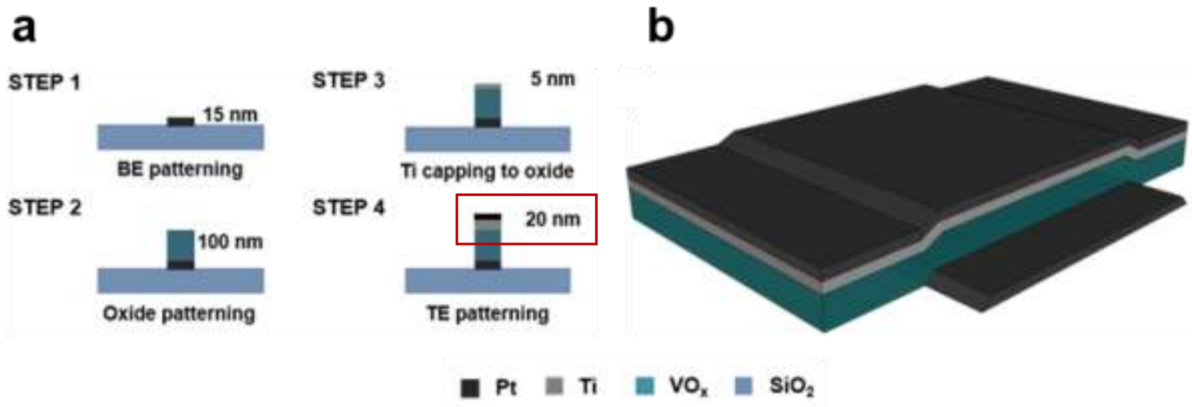

Comment 2

The lateral size of the defined cross bar was not discussed in the manuscript.

Response

We thanks the Reviewer for bringing this to our attention. The device dimensions are included in the manuscript.

Modification

Page 7, Line 286

Devices are fabricated with two different sizes for electrical testing, 4 x 4 µm and 6 x 6 µm.

Comment 3

The annealing conditions were not mentioned in the paper, which is important to avoid the degradation of the electrode.

Response

We are aware that annealing is used to condition the electrode metals and understand the Reviewer’s concern here. However, our films are deposited using electron beam evaporation and they have been tested to render really good conductivity. Additionally, the electrode material used here is platinum (Pt) with adhesion of titanium (Ti). Pt being noble metal degradation is minimal.

From device structure point of view, the aim here was to study amorphous vanadium oxide as functional oxide in a sandwiched metal-oxide-metal or cross-point structure. Annealing would render uniform crystalline vanadium oxide. We have tested that for crystalline vanadium oxide top electrode and bottom electrode gets short due to very porous nature of our crystalline vanadium oxide film due to pinholes and grain boundaries.

Considering the above two points electrode annealing was not used in this case. As it is an important point, the explanation regarding this is added in the revision manuscript in discussion section.

<u>Modification</u>

Page 7 Lines 287-289

The contact electrode used here is Pt, which being a noble metal has minimal degradation over the period. Due to this and to avoid the uniform crystallisation of vanadium oxide in device structure, the normally used electrode annealing step was omitted in our fabrication.

Comment 4

I suggest the authors add the following references to further motivate their study, because such a technique is generally useful for crossbar devices and not limited to VOx: Proceedings of the IEEE 103, 1289 (2015).

<u>Response</u>

We thank the Reviewer for referring us to the above study. The above reference is included in the introduction section.

<u>Modification</u>

Page 10, Line 345

3 Zhou, Y. & Ramanathan, S. Mott Memory and Neuromorphic Devices. *Proceedings of the IEEE.* **103** (8), 1289-1310, (2015).

Page 2, Line 56-57

Multiple switching behaviours have been proposed for resistive switching devices till date.[2,3]

Reviewer 2

Major Concerns:

There are major gaps in the procedures (or in the explanation of the procedures) required to arrive at the conclusions stated in this manuscript. Some of these are concerns with the conclusions drawn in their previously published manuscript (Ref. [3] in Adv. Elec. Mat.). Although this is not a review of a previously published work, this is a criticism of the conclusions stated or referenced in this manuscript as having been drawn from the experimental process followed in this manuscript. I will stick to criticizing the procedures and their rigor, and not the scientific merits of the results. Below I list a few:

Comment 1

The presence of crystalline islands in an amorphous film need not have anything to do with the mechanism of volatile threshold switching. IMT can happen in either amorphous or crystalline films. Moreover, an amorphous film typically has short-range ordering that is not detected by spectroscopic techniques. So you have not used this set of experiments to explain this aspect. While this claim is in your previously published paper, I believe it is a far stretch and should not be claimed here.

<u>Response</u>

First of all we thanks the Reviewer for his time for critical consideration of both this paper and our previously published manuscript.

IMT happens only in the crystalline VO_2 and not in the amorphous VO_2. We have presented the proofs regarding this in our previous publication – Supporting information Figure S2 of the cited reference.[3] Additionally, it is also supported in the literature.[4-6]

About the second point regarding spectroscopic techniques, the focus of this study is to explain the experimental methodology of device fabrication, lamella preparation, and *in situ* biasing in TEM chamber. The representative results uses high resolution TEM micrographs and the corresponding diffraction patterns. While it is very much possible to do the spectroscopic analysis *in situ* using electron energy loss spectroscopy (EELS) in TEM chamber, it was not used this time.

We certainly agree with the Reviewer that the detailed explanation of the previously published results is beyond the scope of this paper. We have removed the detailed explanation in this paper and replaced it with the short summary in the representative results section as presented below.

<u>Modification</u>

Page 6, Lines 201-204

Note: *Once the aforementioned setup is ready data relating to TEM imaging, diffraction patterns, electron diffraction X-ray spectroscopy (EDX), and electron energy loss spectroscopy (EELS) mapping can be collected at different biasing voltages in situ. The representative results are presented in the later section.*

Page 7, Lines 228-231

The strong evidence for the presence of *c*-VO_2 islands in *a*-VO_x devices after biasing at higher voltage helped to prove the resistive switching characteristics (Figure 2 of cited reference[7]) and the switching mechanism (Figure 6 of the cited reference[7]) for asymmetric cross-point devices based on mixed-phased *a*-VO_x.

Comment 2

Are your TEM maps obtained while holding a current or voltage? I would guess not (from the text), but it is not clear. If the TEM maps are not obtained when holding a current/voltage, then it is misleading to call it an in-situ technique.

Response

Yes, Reviewer understanding here is correct. The TEM micrographs are not obtained while holding the constant voltage bias. They are obtained in remanence, immediately after the voltage sweep has finished. For clear and high quality TEM micrographs a focus adjustment is always required just before capturing the image which takes some time. The voltage sweeps are quick and there is no sufficient time to capture a high quality micrograph during the bias.

For the scope of this protocol, it is very much possible to hold the constant voltage bias instead of voltage sweeps and capture TEM micrographs while holding the constant voltage bias, which will be truly an *in situ* as Reviewer is suggesting. Even in that case the complete protocol – the process of device fabrication, lamella preparation, and *in situ* TEM will remain exactly the same from methodology point of view. Just instead on voltage sweeps, we will apply constant voltage which is a tiny modification on the software controlling source-meter.

Even in the constant voltage bias mode there is a tread-off. The energy applied to the sub-100 nm thin lamella with constant voltage will be different at different intervals of time. Due to this the nanostructural changes captured at different time intervals can possibly be different. In our previously published results experimental requirements were of voltage sweeps. For those results, we do partially agree with the Reviewer. However, there are two points we would like to mention. One, we only report of *in situ* TEM micrographs and not any compositional changes which can be possibly different during the voltage sweeps and immediately after the sweep. Second, the formation of *c*-VO_2 islands as a results of voltage sweeps was observed manually to happen during the bias and it being an irreversible change remained the same even after the voltage sweep was finished. Considering these points, the data collected in remanence in this case should be acceptable as *in situ*.

We believe both constant voltage and voltage sweeps have tread offs which are insignificant. For the scope of the protocol explained here, the methodology remains the same regardless of constant voltage or voltage sweep mode.

Modification

Page 7, Line 233

The results show the application of the explained protocol. Here the *in situ* nanostructural changes are captured in remanence of voltage sweeps at different voltages with the high resolution TEM (HRTEM) micrographs and corresponding diffraction patterns.

Page 6, Line 204

Note: *Once the aforementioned setup is ready data relating to TEM imaging, diffraction patterns, electron diffraction X-ray spectroscopy (EDX), and electron energy loss spectroscopy (EELS) mapping can be collected at different biasing voltages in situ by applying either constant voltage or voltage sweeps with the control PC and source meter software as explained in fabrication process and electrical characterisation section.*

Comment 3

Crystal islands do not explain two-step switching. You should have held the voltage at intermediate levels between two switching events to see if indeed only a part of the crystal islands switched. I don't think this was done, and is a major gap in the procedure used to draw the conclusions you have.

Response

We thanks the Reviewer for this point. The experiment he is suggesting was already performed and presented in our previous publication (Figure 2f and inset) electrically.[8] The role of *in situ* TEM results in the mechanism of two-step switching was limited to observing multiple nucleation sites and crystal islands orientated in different directions with respect to the substrate as a result of biasing, which it clearly shows in Figure 7. The complete conclusion in the previous publication was not based on just *in situ* TEM, but it was a combined conclusion of electrical characterisations, *in situ* TEM results, and a support literature where different crystal orientations of VO_2 have been reported to have different IMT temperatures. When the stimulus is voltage instead of temperature, different orientations of VO_2 crystal islands would switch at different voltages.

We believe this point was mainly the part of our previous publication and for the scope of this paper it is not very related. After careful consideration and to avoid confusions, we have removed this discussion from the representative results section and replaced it with a short summary.

Modification

Page 7, Lines 228-231

The strong evidence for the presence of *c*-VO_2 islands in *a*-VO_x devices after biasing at higher voltage helped to prove the resistive switching characteristics (Figure 2 of cited reference[7]) and the switching mechanism (Figure 6 of the cited reference[7]) for asymmetric cross-point devices based on mixed-phased *a*-VO_x.

Minor Concerns:

The English usage in the manuscript can be improved. And there are a few mistakes (for instance, you wrote "nucleation sights" instead of "nucleation sites", also found in the earlier published paper).

Response

We thank the reviewer for bringing it to our attention. The spelling typos have been carefully checked and corrected throughout the revised manuscript.

Another minor concern is self-plagiarism. Some of the figure panels, and in some cases entire figures have been reproduced from your earlier published paper. And so are some parts of the text. Please revise all the text, and I suggest change the figures in some minor ways (orientation, ordering, coloring, etc.) or you will have to obtain permission to reuse the figures. The Editor should be able to assist you here.

Response

We again thanks the Reviewer for their careful observations. This point has been discussed with the Editor and the copyright permissions are submitted. Figures and text have been cited appropriately where required to address the self-plagiarism issue.

References

[1] F. Pan, S. Gao, C. Chen, C. Song, F. Zeng, *Materials Science and Engineering: R: Reports* **2014**, *83*, 1.

[2] Y. Zhou, S. Ramanathan, *Proceedings of the IEEE* **2015**, *103*, 1289.

[3] R. K. Yafarov, *Semiconductors* **2018**, *52*, 137.

[4] J. A. Rupp, M. Querré, A. Kindsmüller, M.-P. Besland, E. Janod, R. Dittmann, R. Waser, D. J. Wouters, *Journal of Applied Physics* **2018**, *123*, 044502.

[5] J. Rupp, R. Waser, D. Wouters, "Threshold Switching in Amorphous Cr-doped Vanadium Oxide for New Crossbar Selector", presented at *Memory Workshop (IMW), 2016 IEEE 8th International*, **2016**.

[6] M. Taha, S. Walia, T. Ahmed, D. Headland, W. Withayachumnankul, S. Sriram, M. Bhaskaran, *Scientific Reports* **2017**, *7*, 17899.

[7] S. Nirantar, E. Mayes, M. A. Rahman, T. Ahmed, M. Taha, M. Bhaskaran, S. Walia, S. Sriram, *Advanced Electronic Materials* **2019**, 1900605.

[8] S. Nirantar, E. Mayes, M. A. Rahman, T. Ahmed, M. Taha, M. Bhaskaran, S. Walia, S. Sriram, *Advanced Electronic Materials* **2019**, *0*, 1900605.

JOHN WILEY AND SONS LICENSE
TERMS AND CONDITIONS

Nov 13, 2019

This Agreement between RMIT University -- Shruti Nirantar ("You") and John Wiley and Sons ("John Wiley and Sons") consists of your license details and the terms and conditions provided by John Wiley and Sons and Copyright Clearance Center.

License Number	4707400566098
License date	Nov 13, 2019
Licensed Content Publisher	John Wiley and Sons
Licensed Content Publication	Advanced Electronic Materials
Licensed Content Title	In Situ Nanostructural Analysis of Volatile Threshold Switching and Non-Volatile Bipolar Resistive Switching in Mixed-Phased a-VOx Asymmetric Crossbars
Licensed Content Author	Shruti Nirantar, Edwin Mayes, Md. Ataur Rahman, et al
Licensed Content Date	Aug 26, 2019
Licensed Content Volume	0
Licensed Content Issue	0
Licensed Content Pages	9
Type of use	Journal/Magazine
Requestor type	Author of this Wiley article
Is the reuse sponsored by or associated with a pharmaceutical or medical products company?	no

Format	Electronic
Portion	Figure/table
Number of figures/tables	1
Original Wiley figure/table number(s)	Figure 4 and Figure 1 in Supporting Information
Will you be translating?	No
Circulation	30 - 99
Title of new article	Fabrication process and in situ nanostructural analysis methodology of volatile threshold switching in mixed-phased a-VOx based asymmetric crossbars
Publication the new article is in	The Journal of Visualized Experiment
Publisher of new article	JoVE
Author of new article	Shruti Nirantar, Edwin Mayes, and Sharath Sriram
Expected publication date of new article	Feb 2020
Estimated size of new article (pages)	1
Requestor Location	RMIT University GPO Box 2476 Melbourne, Victoria (VIC) 3001 Australia Attn: RMIT University
Publisher Tax ID	EU826007151
Total	0.00 AUD

Terms and Conditions

TERMS AND CONDITIONS

license or interest to any trademark, trade name, service mark or other branding ("Marks") of WILEY or its licensors is granted hereunder, and you agree that you shall not assert any such right, license or interest with respect thereto

- NEITHER WILEY NOR ITS LICENSORS MAKES ANY WARRANTY OR REPRESENTATION OF ANY KIND TO YOU OR ANY THIRD PARTY, EXPRESS, IMPLIED OR STATUTORY, WITH RESPECT TO THE MATERIALS OR THE ACCURACY OF ANY INFORMATION CONTAINED IN THE MATERIALS, INCLUDING, WITHOUT LIMITATION, ANY IMPLIED WARRANTY OF MERCHANTABILITY, ACCURACY, SATISFACTORY QUALITY, FITNESS FOR A PARTICULAR PURPOSE, USABILITY, INTEGRATION OR NON-INFRINGEMENT AND ALL SUCH WARRANTIES ARE HEREBY EXCLUDED BY WILEY AND ITS LICENSORS AND WAIVED BY YOU.

- WILEY shall have the right to terminate this Agreement immediately upon breach of this Agreement by you.

- You shall indemnify, defend and hold harmless WILEY, its Licensors and their respective directors, officers, agents and employees, from and against any actual or threatened claims, demands, causes of action or proceedings arising from any breach of this Agreement by you.

- IN NO EVENT SHALL WILEY OR ITS LICENSORS BE LIABLE TO YOU OR ANY OTHER PARTY OR ANY OTHER PERSON OR ENTITY FOR ANY SPECIAL, CONSEQUENTIAL, INCIDENTAL, INDIRECT, EXEMPLARY OR PUNITIVE DAMAGES, HOWEVER CAUSED, ARISING OUT OF OR IN CONNECTION WITH THE DOWNLOADING, PROVISIONING, VIEWING OR USE OF THE MATERIALS REGARDLESS OF THE FORM OF ACTION, WHETHER FOR BREACH OF CONTRACT, BREACH OF WARRANTY, TORT, NEGLIGENCE, INFRINGEMENT OR OTHERWISE (INCLUDING, WITHOUT LIMITATION, DAMAGES BASED ON LOSS OF PROFITS, DATA, FILES, USE, BUSINESS OPPORTUNITY OR CLAIMS OF THIRD PARTIES), AND WHETHER OR NOT THE PARTY HAS BEEN ADVISED OF THE POSSIBILITY OF SUCH DAMAGES. THIS LIMITATION SHALL APPLY NOTWITHSTANDING ANY FAILURE OF ESSENTIAL PURPOSE OF ANY LIMITED REMEDY PROVIDED HEREIN.

- Should any provision of this Agreement be held by a court of competent jurisdiction to be illegal, invalid, or unenforceable, that provision shall be deemed amended to achieve as nearly as possible the same economic effect as the original provision, and the legality, validity and enforceability of the remaining provisions of this Agreement shall not be affected or impaired thereby.

- The failure of either party to enforce any term or condition of this Agreement shall not constitute a waiver of either party's right to enforce each and every term and condition of this Agreement. No breach under this agreement shall be deemed waived or excused by either party unless such waiver or consent is in writing signed by the party granting such waiver or consent. The waiver by or consent of a party to a breach of any provision of this Agreement shall not operate or be construed as a waiver of or consent to any other or subsequent breach by such other party.

- This Agreement may not be assigned (including by operation of law or otherwise) by you without WILEY's prior written consent.

- Any fee required for this permission shall be non-refundable after thirty (30) days from receipt by the CCC.

- These terms and conditions together with CCC's Billing and Payment terms and conditions (which are incorporated herein) form the entire agreement between you and WILEY concerning this licensing transaction and (in the absence of fraud) supersedes all prior agreements and representations of the parties, oral or written. This Agreement may not be amended except in writing signed by both parties. This Agreement shall be binding upon and inure to the benefit of the parties' successors, legal representatives, and authorized assigns.

- In the event of any conflict between your obligations established by these terms and conditions and those established by CCC's Billing and Payment terms and conditions, these terms and conditions shall prevail.

- WILEY expressly reserves all rights not specifically granted in the combination of (i) the license details provided by you and accepted in the course of this licensing transaction, (ii) these terms and conditions and (iii) CCC's Billing and Payment terms and conditions.

- This Agreement will be void if the Type of Use, Format, Circulation, or Requestor Type was misrepresented during the licensing process.

- This Agreement shall be governed by and construed in accordance with the laws of the State of New York, USA, without regards to such state's conflict of law rules. Any legal action, suit or proceeding arising out of or relating to these Terms and Conditions or the breach thereof shall be instituted in a court of competent jurisdiction in New York County in the State of New York in the United States of America and each party hereby consents and submits to the personal jurisdiction of such court, waives any objection to venue in such court and consents to service of process by registered or certified mail, return receipt requested, at the last known address of such party.

WILEY OPEN ACCESS TERMS AND CONDITIONS

Wiley Publishes Open Access Articles in fully Open Access Journals and in Subscription journals offering Online Open. Although most of the fully Open Access journals publish open access articles under the terms of the Creative Commons Attribution (CC BY) License only, the subscription journals and a few of the Open Access Journals offer a choice of Creative Commons Licenses. The license type is clearly identified on the article.

The Creative Commons Attribution License

The Creative Commons Attribution License (CC-BY) allows users to copy, distribute and transmit an article, adapt the article and make commercial use of the article. The CC-BY license permits commercial and non-

Creative Commons Attribution Non-Commercial License

The Creative Commons Attribution Non-Commercial (CC-BY-NC)License permits use, distribution and reproduction in any medium, provided the original work is properly cited and is not used for commercial purposes.(see below)

Creative Commons Attribution-Non-Commercial-NoDerivs License

The Creative Commons Attribution Non-Commercial-NoDerivs License (CC-BY-NC-ND) permits use, distribution and reproduction in any medium, provided the original work is properly cited, is not used for commercial purposes and no modifications or adaptations are made. (see below)

Use by commercial "for-profit" organizations